Boron removal from water by adsorption onto activated carbon prepared from palm bark: kinetic, isotherms, optimisation and breakthrough curves modeling

Abir Melliti, Jamel Kheriji, Hanen Bessaies and Béchir Hamrouni

ABSTRACT

The occurrence of boron in water and its inefficient removal are the key issue in desalination and water treatment. Adsorption by fixed-bed column is usually used to remove mineral and organic contaminants from the aqueous phase. The adsorption of the boron onto activated carbon, prepared from palm bark, is studied. Batch adsorption experiments are developed to determine the equilibrium time and the best isotherm model. The kinetic adsorption data can be described by the second-order equation. Among the adsorption isotherm models, Langmuir and Sips models give better fit of the equilibrium data. The calculated thermodynamic parameters show that the boron adsorption is exothermic in nature. The effects of inlet boron concentration, feed flow rate and weight of activated carbon on the fixed-bed adsorption are determined by two-level factorial experimental design. Breakthrough and saturation times are higher at high adsorbent weight and low flow rates. The increase of boron initial concentration decreases breakthrough and saturation times. The volume treated per gram of activated carbon is higher at lower initial concentrations and at higher adsorbent weight. Compared to other models, the Yan model fits better the experimental data of the breakthrough curves with R^2 of 0.993.

Key words | adsorption, batch process, boron, experimental design, fixed-bed column, palm bark activated carbon

Abir Melliti
Jamel Kheriji (corresponding author)
Hanen Bessaies
Béchir Hamrouni
Research Laboratory of Desalination and Water Treatment,
Faculty of Sciences, University of Tunis El Manar,
2092 Tunis,
Tunisia
E-mail: *jamel.khriji@gmail.com*

INTRODUCTION

Naturally present in the environment, boron is a chemical element, which can combine with oxygen or other elements in compounds that one names borates. The latter are present in waters, sedimentary rocks or in certain soils. In water, boron exists in the form of boric acid $B(OH)_3$. In sea water, its concentration reaches approximately 5 mg L^{-1}. Boron is known as one of the essential elements for living plants, animals and humans. However, in greater amounts, boron can be harmful to human, animal and plant life. In humans, the sign of acute toxicity includes nausea, vomiting, diarrhea, dermatitis and lethargy (Shaaban 2010). The World Health Organization guidelines for drinking water quality proposed 2.4 mg L^{-1} as standard for boron in drinking water (Liu *et al.* 2009).

Boron is one of the elements most problematic in water. There does not exist any effective method for its elimination. Main processes that have been studied for boron removal are chemical precipitation, adsorption (Lyu *et al.* 2017), reverse osmosis (Dydo *et al.* 2012) and electrodialysis. Among these methods, an adsorption method is promising for the boron removal because it requires simple operating conditions and can be applied for the water treatment at low concentrations. For this reason, numerous studies on the boron adsorption have been conducted so far using various adsorbents such as natural and synthesized clay minerals, ion-exchange resins, activated carbons, metal oxides, cellulose and ashes.

The aim of this study was to prepare activated carbon from palm tree and to carry out the structural, functional and surface chemistry of the prepared adsorbent. We investigated the adsorption behavior of boron onto this adsorbent. Kinetic and isotherm studies were made. Thermodynamic parameters, and batch and column capacities were calculated. Thomas, Bohart–Adams, Yan and Yoon–Nelson models were applied to experimental data obtained from the column study. A fixed-bed system was determined

doi: 10.2166/wst.2020.107

in laboratory scale through a two-level factorial experimental design. The influences of initial boron concentration, adsorbent dosage and volumetric flow rate were studied regarding breakthrough and saturation times, volume treated and fractional bed utilization.

MATERIALS AND METHODS

Materials

The model aqueous solution for the experiments was prepared by dissolving an appropriate amount of boric acid (Acros Organics) in distilled water to the concentration of 100 mg L^{-1}. All other solutions used were freshly prepared for each experimental run.

Preparation of activated carbon from palm bark

Palm tree bark was used for preparation of granular activated carbon, and was obtained from the oasis of Gabes, Tunisia. It was washed with hot distilled water to remove dust-like impurities. After that, it was dried in an oven at a temperature of 105 °C for 24 hours and then crushed and sieved to the desired particle size (1–2 mm). The carbonization process was performed in a muffle furnace at 700 °C under inert atmosphere, with a ramping rate of 10 °C min^{-1} (Foo & Hameed 2012). The sample was held at the carbonization temperature for 2 hours. The carbon produced was soaked in a potassium hydroxide (KOH) solution with an impregnation ratio of 1:1. The mixture was then dehydrated in an oven overnight at 105 °C to remove moisture and then activated under the same conditions as carbonization, to a final temperature of 600 °C. After activation, the samples were cooled to room temperature. Then, they were washed sequentially several times with hot distilled water (70 °C) until the pH of the washing solution reached 6–7. Finally, samples were dried in an oven at 110 °C for 24 hours and then stored in plastic containers (Ahmad & Hameed 2010).

Characterization of activated carbon

The pore structural characteristic of this activated carbon was investigated by nitrogen adsorption using an automatic Micromeritics ASAP-2020 volumetric adsorption analyzer. Prior to analysis, the sample was degassed for 4 h under vacuum at 423 K. After degassing, the sample was transferred to the analysis system where it was cooled in liquid nitrogen. Chemical characterization of surface functional groups was undertaken using pressed potassium bromide (KBr) pellets containing 5% of carbon sample by a Fourier transform infrared (FTIR) spectrometer (FTIR-2000, Perkin Elmer). The FTIR spectra were analyzed between 4,000 and 400 cm^{-1}.

Batch adsorption

Adsorption batch tests were carried out in a thermostatic bath of Grant type with adjustable stirring speed and temperature. In this bath, 100 mL of boron solution was prepared in distilled water at 25 °C at different concentrations. One gram of activated carbon was added into the batch at a stirring speed and at a well-defined temperature. The pH of the solutions was natural (pH 5.5). Aqueous samples were taken from the solution and the concentrations were analyzed. The time range was 5–60 minutes. All samples were filtered prior to the analysis to minimize the interference of the carbon fines in the analysis. Boron concentration of all samples was determined by a UV-visible spectrophotometer (VWR UV-1600PC) at wavelength of 410 nm.

Kinetic modeling

To investigate the mechanism of boron adsorption on activated carbon, the pseudo-first-order (Equation (1)) (Lagergren 1898), the pseudo-second-order (Equation (2)) (Ho & McKay 1999), and the intraparticle diffusion (Equation (3)) (Danmaliki & Saleh 2016) models were employed with the following equations:

$$q_t = q_e(1 - \exp(-k_1 t)) \quad (1)$$

$$\frac{dq_t}{dt} = k_2(q_e - q_t)^2 \quad (2)$$

$$q_t = k_{dif} t^{1/2} + C \quad (3)$$

where q_t is the amount of boron adsorbed (mg g^{-1}) at time t (min), q_e (mg g^{-1}) is the equilibrium adsorption capacity per gram dry weight of the adsorbent, k_1 is the pseudo-first-order rate constant for the boron adsorption process (min^{-1}), k_2 is the pseudo-second-order rate constant (g mg^{-1} min^{-1}), k_{dif} is the intraparticle diffusion rate constant (mg g^{-1} $min^{-0,5}$), and C is the intercept.

Adsorption isotherms

Numerous theories and models have been developed to interpret the different types of isotherms; the resulting

equations can be used to predict quantities adsorbed from a minimum of experimentation.

The isotherms equations of Langmuir (Equation (4)), Freundlich (Equation (5)) Dubinin–Radushkevich (Equation (6)) and Temkin (Equation (7)) were used in this study, as well as the equation of the Sips model (Equation (8)).

$$q_e = \frac{q_m K_L C_e}{1 + K_L C_e} \tag{4}$$

$$q_e = K_F C_e^{1/n} \tag{5}$$

$$q_e = q_D \exp(-K_D \varepsilon^2) \tag{6}$$

$$q_e = B \ln(K_T C_e) \tag{7}$$

$$q_e = \frac{q_s K_s C_e^{n_s}}{1 + K_s C_e^{n_s}} \tag{8}$$

where q_e (mg g^{-1}) is the equilibrium adsorption capacity per gram dry weight of the adsorbent, K_L is the Langmuir constant related to the free energy of adsorption (L mg^{-1}), C_e is the solute concentration at equilibrium (mg L^{-1}), K_F and n are Freundlich constants which give a measure of adsorption capacity and adsorption intensity, ε is Polanyi potential, q_D is the adsorption capacity (mol g^{-1}), K_D is the Dubinin–Radushkevich constant related to adsorption energy (mol^2 kJ^{-2}), $B = RT/b$ (R is the ideal gas constant (8.314 J K^{-1} mol^{-1}), T is the absolute temperature (K), b is the Temkin constant related to heat of sorption (J mol^{-1})), K_T is the Temkin isotherm constant (L g^{-1}), q_s (mg g^{-1}) is the Sips maximum uptake of boron per unit mass of adsorbent, K_s (L mg^{-1}) is the Sips constant related to energy of adsorption and n is the Sips parameter that characterizes the system heterogeneity.

Adsorption thermodynamics

The thermodynamics of the adsorption process depends on the system total energy change (ΔH°), Gibbs free energy change (ΔG°) and entropy change (ΔS°). By evaluating these parameters, it is possible to decide whether the process is spontaneous or not. Reactions happen spontaneously at a given temperature if ΔG° is a negative value. The free energy of an adsorption process is associated with the equilibrium constant by the following (Saha & Chowdhury 2011):

$$\Delta G^\circ = -RT \ln K \tag{9}$$

$$\Delta G^\circ = \Delta H^\circ - T\Delta S^\circ \tag{10}$$

where ΔG° is the free energy exchange (kJ mol^{-1}), K is a thermodynamic equilibrium constant obtained with:

$$\ln K = \frac{-\Delta H^\circ}{RT} + \frac{\Delta S^\circ}{R} \tag{11}$$

Fixed-bed column studies

Experimental procedure

The fixed-bed column studies were performed using a laboratory-scale glass column with an internal diameter of 1.2 cm and a length of 50 cm. The length of activated carbon bed was varied according to the amount of adsorbent. The boron solution of known concentrations was pumped upward through the column at a desired flow rate controlled by a peristaltic pump (Ismatec BVP-Z). The boron solutions at the outlet of the column were collected at regular time intervals and the concentration was measured using a UV-visible spectrophotometer at 410 nm. Each experiment used different volumes of inlet effluent depending on the saturation time at certain experimental condition. All the experiments were performed at 25 °C using deionized water at the native pH of the solution (5.5). The breakthrough curves were obtained by continuous monitoring. Deionized water at a flow rate of 3 mL min^{-1} was introduced into the column, before each experiment, in order to humidify the porosity of the activated carbon.

Experimental design and surface response methods

The fractional factorial design is used to reduce a number of experiments when there are many factors included in the study. So, this design is a way to simplify the full factorial design because it reduces the number of experiments required (Anderson & Whitcomb 2005).

In this study the influence of three operation variables (factors) on a parameter (response), full factorial design (2^3) (Zuorro 2015), was applied: initial boron concentration (C_0), weight (W) of adsorbent and volumetric feed flow rate (Q).

Four response factors were evaluated: breakthrough time (t_b), saturation time (t_s), treated volume (V_s) and fraction bed utilization (FBU). Breakthrough time defines the time to reach 5% of initial concentration. Saturation time presents the time to reach 95% of initial concentration of boron. Data were analysed using the software Statistica 8 (Bakkal *et al.* 2015).

Breakthrough curves modeling

Successful design of a column adsorption process requires prediction of the breakthrough curve for the effluent. The maximum adsorption capacity of an adsorbent is also needed in design. Mathematical breakthrough curve models were used to predict a fixed-bed column performance and to calculate kinetic constants and uptake capacities (Cruz-Olivares *et al.* 2013). Three analytical breakthrough curve models were employed to fit the experimental data: Thomas, Bohart–Adams, Yoon–Nelson and Yan models.

The Bohart–Adams model (Bohart & Adams 1920) model established the fundamental equations describing the relationship between C_e/C_0 and t in a continuous system. The Bohart–Adams model was used for the description of the initial part of the breakthrough curve. The expression of this model is defined in Equation (12):

$$\frac{C_e}{C_0} = \exp\left((K_{BA}.C_0.t) - \left(\frac{K_{BA}N_0Z}{v}\right)\right) \tag{12}$$

where K_{BA} (L mg^{-1} min^{-1}) is the kinetic constant, Z (cm) is the bed depth of column, N_0 (mg L^{-1}) is the saturation concentration and v is the linear flow rate (cm min^{-1}).

The Thomas model (Thomas 1944) assumes plug flow behaviour in the bed. This model is one of the most general and widely used to describe the performance theory of the sorption process in fixed-bed column. The expression is the following:

$$\frac{C_e}{C_0} = \frac{1}{1 + \exp\left(\frac{K_{Th}}{Q}(q_0.m - C_0.V)\right)} \tag{13}$$

where K_{Th} is the Thomas model constant (mL min^{-1} mg^{-1}), q_0 is the adsorption capacity of adsorbent (mg g^{-1}), m is the mass of adsorbent (g), and V is the volume of treated solution (L).

Yoon and Nelson developed this model which assumes that the rate of decrease in the probability of adsorption for each adsorbate molecule is proportional to the breakthrough of the adsorbent. The Yoon–Nelson equation concerning a single component system is expressed as:

$$\frac{C_e}{C_0} = \frac{1}{1 + \exp\left(K_{YN}(t_{50} - t)\right)} \tag{14}$$

where K_{YN} is the constant of Yoon and Nelson (s^{-1}), t_{50} is the time required to maintain 50% of the initial adsorbent in minutes.

It is important to specify that the expression of the Yoon and Nelson model is mathematically analogous to the equation which represents the Thomas model.

The Yan model was proposed (Yan & Viraraghavan 2003) in order to minimize the error that results from the use of the Thomas model, especially at very small and very large operation times. The Yan model can be formulated as follows:

$$\frac{C_t}{C_0} = 1 - \frac{1}{1 + \left(\frac{C_0.Q.t}{q_Y m}\right)a_Y} \tag{15}$$

where q_Y is the amount of solute adsorbed (mg g^{-1}) and a_Y is the constant of the Yan model.

RESULTS AND DISCUSSION

Characterization of adsorbent

The chemical surface groups of the raw material and activated carbon were studied from the FTIR spectra. The FTIR spectra showed that the intensity of all the peaks decreased significantly for the activated carbon compared to its precursor. This is associated with the destruction of intermolecular bonds during thermal and chemical activation. For the FTIR spectra of activated carbon, it has been reported that the band at around 3,384.24 cm^{-1} can be attributed to the stretching vibration of O-H of hydroxyl functional groups (Torrellas *et al.* 2015); a reduced intensity for the prepared activated carbon was maybe due to the decrease in volatile matter and moisture content (Sulaiman *et al.* 2018). The bands at 2,353.14 and 2,328.51 cm^{-1} have been allocated to the C≡C stretch (Islam *et al.* 2015). The peak at around 1,734 cm^{-1} corresponds to the stretching vibration of C=O of the carbonyls for the raw material, and the absence of this peak for the activated carbon indicated numerous removals of aromatic and aliphatic bonds during the thermochemical process (Mahmood *et al.* 2017). The peak detected at 1,633.58 cm^{-1} corresponded to stretching vibrations of C=C and a weakened peak for a reduction in the aromatic content contrasted with the precursor (Hsu *et al.* 2014). The peaks occurring at 1,358.17 and 1,060.28 cm^{-1} were all attributed to oxygen functionalities such as C-O stretching vibrations and C-O bending vibrations of primary alcohols (Islam *et al.* 2015).

The elemental analysis of activated carbon was carried out using GmbH Elementar. Results show that the activated carbon is composed of 67.58% carbon, 2.16% hydrogen, 29.01% oxygen and 1.22% nitrogen.

In order to evaluate the surface charge of activated carbon, the pH at the point of zero charge (pH_{pzc}) was determined and the results showed that the pH_{pzc} value was 7.2. This value indicates the neutral character of the surface. The pH_{pzc} value of activated carbon suggests that its surface can have a predominance of negative charges, since for $pH_{solution} > pH_{pzc}$ the surface tends to be predominantly positive, while for $pH_{solution} < pH_{pzc}$ the surface tends to be predominantly negative.

The nitrogen adsorption–desorption isotherm of activated carbon corresponded to a type I isotherm, which indicates the presence of the microporous structure. The average pore diameter of the sample is 21. 29 Å, confirming the existence of a microporous structure with a surface area of 836.44 $m^2\,g^{-1}$. The large specific surface area is helpful for the adsorbate molecules approach to the adsorbent-active sites, which can enhance the adsorption efficiency.

Kinetic studies

To study the mechanism of boron adsorption by activated carbon, three most frequently used kinetic models, namely, pseudo-first-order (Equation (1)), pseudo-second-order (Equation (2)) and intraparticle diffusion model (Equation (3)), were used to assess the adsorption of boron. The derived model parameters from fittings of the data in Figure 1, including the kinetic constant (k), square of correlation coefficient (R^2), and equilibrium adsorption capacity (q_e), are shown in Table 1.

The R^2 value of the pseudo-second-order model (0.954) was closer to 1.0 and greater than that of the pseudo-first-order model (0.899). On the other hand, the q_e values calculated from the pseudo-second-order model were nearer to the observed experimental ones (q_{exp}). These results indicated that the adsorption of boron on activated carbon was well fitted to the pseudo-second-order kinetic model compared with the first-order model. It can be concluded that the pseudo-second-order kinetic model gives a good correlation for the adsorption of boron on activated carbon.

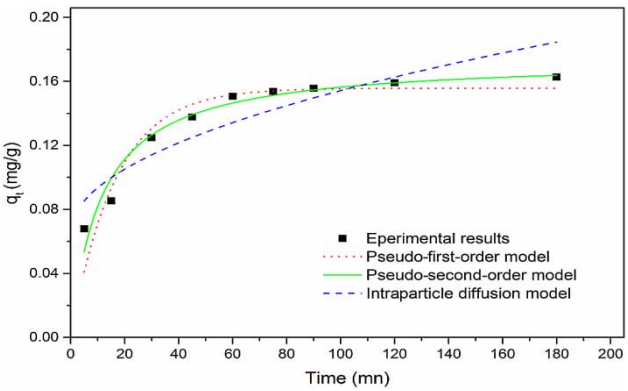

Figure 1 | Boron adsorption onto activated carbon non-linear kinetic curves.

Table 1 | Parameters and determination coefficients of pseudo-first-order, pseudo-second-order and intraparticle diffusion models

Pseudo-first-order model	q_e (mg g^{-1})	1.556
	k_1 (min^{-1})	0.061
	R^2	0.899
	χ^2	1.359×10^{-4}
Pseudo-second-order model	q_e (mg g^{-1})	0.174
	k_2 (g mg^{-1} min^{-1})	0.509
	R^2	0.954
	χ^2	6.209×10^{-5}
Intraparticle diffusion model	C (mg g^{-1})	0.065
	K_{dif} (mg $L^{-1/2}$ $min^{-1/2}$)	0.008
	R^2	0.817
	χ^2	2.454×10^{-4}

The intraparticle diffusion model was used to determine the rate-limiting step of the adsorption kinetics (Georgieva *et al.* 2015). This model accepts that the adsorption mechanism happens through the diffusion of adsorbate molecules into the pores of adsorbent material. The plots for q_t versus $t^{1/2}$ are shown in Figure 2.

If the plot of q_t versus $t^{1/2}$ gives a straight line, then the adsorption process was controlled by intraparticle diffusion.

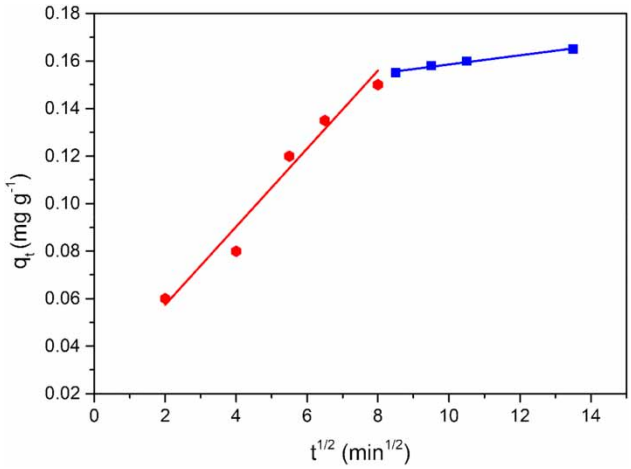

Figure 2 | Intraparticle diffusion plot of the adsorption kinetics of boron onto activated carbon.

But, if the data show multi-linear plots, then two or more steps affect the adsorption process.

As can be seen in Figure 2, plots were separated into two linear regions. The first stage indicates a curve generally ascribed to boundary layer diffusion effects or external mass transfer effects. The second stage is the gradual adsorption period with control of the intraparticle diffusion. The deviation of straight lines from the origin may be due to difference in rate of mass transfer in the initial and final stages of adsorption. Additionally, the deviation of the straight line from the origin shows that the pore diffusion was not the only rate-controlling step for the boron adsorption process (Kavitha 2016).

Adsorption equilibrium isotherms

Adsorption isotherm studies play an important role in the predictive modeling procedure for the analysis and design of an adsorption process. In this study, five adsorption isotherm models (Langmuir (Equation (4)), Freundlich (Equation (5)), Dubinin–Radushkevich (Equation (6)), Temkin (Equation (7)) and Sips (Equation (8))) were applied to the experimental data by the software OriginPro8.6. Figure 3 shows the non-linear plots of isotherm models fitted to these experimental data. The values of isotherm parameters are given in Table 2.

From the correlation coefficients obtained for the different models studied, it can be noticed that the Langmuir and Sips models were those that can give a good fit to the experimental data obtained.

The small difference between the values of R^2 obtained for these two isothermal models led us to use another statistical tool, which is the chi-square test (χ^2). This statistical quantity was given by the software used; its mathematical formula is as follows (Abdu *et al.* 2014):

$$\chi^2 = \sum \frac{(q_{e,\exp} - q_{e,\mathrm{cal}})2}{q_{e,\mathrm{cal}}} \tag{16}$$

where q_e and $q_{e,cal}$ are, respectively, experimental and calculated equilibrium adsorption capacities. The values of χ^2 for the Langmuir and Sips models are, respectively: 2.87×10^{-3} and 3.04×10^{-3}. The highest R^2 and the lowest χ^2 values are obtained for the Langmuir model, which indicates that this model is the most suitable model.

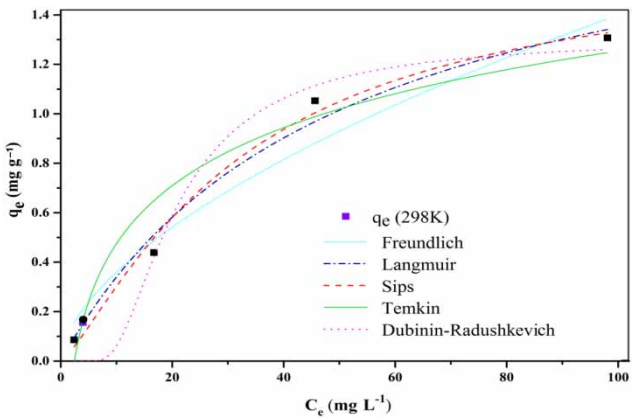

Figure 3 | Adsorption isotherm of boron onto activated carbon and non-linear adjustments of Langmuir, Freundlich, Temkin, Dubinin–Radushkevich and Sips models.

Table 2 | Parameters and determination coefficients of Langmuir, Freundlich, Temkin, Dubinin–Radushkevich and Sips isotherm models

Isotherms	Parameters (25 °C)	
Freundlich	K_F (L mg^{-1})	0.082
	n	1.580
	R^2	0.97
Langmuir	K_L (L mg^{-1})	0.015
	q_m (mg g^{-1})	2.377
	R^2	0.991
Sips	K_s (L mg^{-1})	0.011
	q_s (mg g^{-1})	1.59 ± 0.3
	n_s	0.836
	R^2	0.990
Temkin	B (J mol^{-1})	0.362
	K_T (L mg^{-1})	0.384
	R^2	0.930
Dubinin–Radushkevich	q_D (mg g^{-1})	1.355
	K_D (mol^2 KJ^{-2})	0.152
	E[a] (KJ mol^{-1})	1.813
	R^2	0.959

[a] $E = \frac{1}{\sqrt{2K_D}}$ is the free energy of adsorption (KJ mol^{-1}).

Adsorption thermodynamics

The plot of $\ln K_D$ versus 1/T was linear with the slope and intercept giving the values of ΔH° and ΔS° respectively. The constants of the thermodynamics are shown in Table 3.

An increase in the value of ΔG° depending on the temperature indicates that the adsorption process is more favorable at lower temperatures. The negative values for enthalpy change, ΔH°, confirm the boron adsorption was an exothermic process. Negative entropy change, ΔS°, values show that the solid–liquid interface decreases randomly during the adsorption.

Table 3 | Thermodynamic parameters of boron adsorption

Temperature (°C)	K	ΔG_T° (KJ mol^{-1})	ΔH_T° (KJ mol^{-1})	ΔS_T° (KJ mol^{-1} K^{-1})
10	0.536	1.467	− 23.521	− 0.087
20	0.449	1.950		
25	0.393	2.314		
30	0.316	2.902		
50	0.162	4.888		

Fixed-bed column studies

A two-level full factorial experimental design had been conducted to evaluate the effects of three variables on four different response factors. The experimental data was analyzed using Statistica 8. Table 4 shows the experimental conditions used and the results obtained from each experiment. Analysis of variance (ANOVA) for the four response factors are shown in Table 5.

ANOVA presents successful evidences such as high determination coefficients for all response factors, with values up to 0.96 as stated in Table 5. The *p*-value <0.05 indicates if a factor or interaction is significant in the adsorption process (95% confidence level). All analysis for each response is presented in the following four subsections.

The breakthrough time analysis

The breakthrough time (t_b) is the first response factor that was calculated and represents the time required to detect 5% of the contaminant at the column outlet. *P*-values <0.05 of the main effects (initial concentration, adsorbent weight and flow rate) indicate they are all significant (Table 5). The adsorbent weight shows the lowest *p*-value among the three variables. This result indicates breakthrough time is highly affected by feed adsorbent weight.

Table 4 | Experimental design 2^3 matrix and responses for the boron adsorption by activated carbon

Experimental conditions			Response factors			
C_0 (mg L^{-1})	W (g)	Q (mL min)	t_b (min)	t_s (min)	V_s (mL g^{-1})	FBU
7	7	7	12.5	40	40	0.132
3	3	7	4	18	42	0.432
3	7	7	18	56	56	0.417
7	3	7	2	14	32.66	0.554
7	7	3	15	47	20.14	0.511
7	3	3	6	23	23	0.699
5	5	5	8	27	27	0.423
5	5	5	9	28	28	0.424
5	5	5	8	28	28	0.428
3	7	3	24	65	27.85	0.5
3	3	3	10	34	34	0.46

Table 5 | *P*-values of the main effects and interactions of the response factors on the 2^3 experimental design

		Response factors			
		t_b (min)	t_s (min)	V_s (mL g^{-1})	FBU
Main effect	C_0	0.036	0.069	0.043	0.508
	W	0.002	0.003	0.459	0.008
	Q	0.049	0.011	0.012	0.006
Interaction	$C_0 * W$	0.269	0.394	0.833	0.006
	$C_0 * Q$	0.453	0.675	0,683	0.026
	$Q * W$	0.832	0.675	0.114	0.073
R-square		0.946	0.921	0.890	0.960

The breakthrough time was related to the input variables in terms of real values according to the following equation:

$$t_b = 10.590 - 2.562\,C_0 + 5.937\,W - 2.312\,Q - 1.062\,C_0W + 0.687\,C_0Q + 0.187\,QW \quad (17)$$

The high value of R^2 (0.946) indicates the regression model fits the experimental data well. Response surfaces of the breakthrough time were constructed to study the relationship between independent variables and their interactive effects on the response in three-dimensional planes as shown in Figure 4.

The breakthrough time increases with increasing adsorbent weight due to their positive effects in the regression model of t_b (Equation (17)). Shorter breakthrough times at lower adsorbent weight might be attributed to limited number of adsorption sites on the activated carbon leading to earlier t_b (García-Mateos *et al.* 2015; Mondal *et al.* 2016). It is evident from the figure also that breakthrough time decreased with an increase in the initial boron concentration. This happened because a large number of sorption sites get occupied with an increase in C_0. As the value of C_0 increases, mass transfer is apparent to control the resistance presented by the solution. The same was reported by Shaidan *et al.* (2012). On the other hand, an increment of the flow rate decreases the residence time in the column bed. Thus, shorter breakthrough times are observed at higher flow rates (Meng *et al.* 2013).

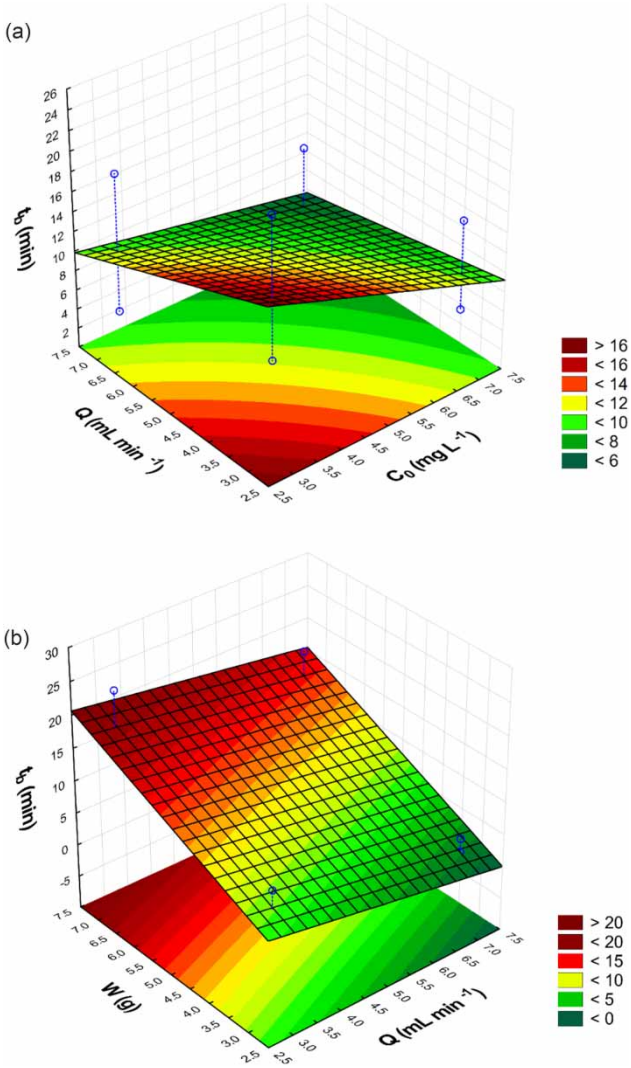

Figure 4 | Response surfaces of the breakthrough time of fixed-bed boron adsorption onto activated carbon as function of: (a) initial boron concentration and flow rate (W = 5 g); and (b) adsorbent dosage and flow rate ($C_0 = 5$ mg L^{-1}).

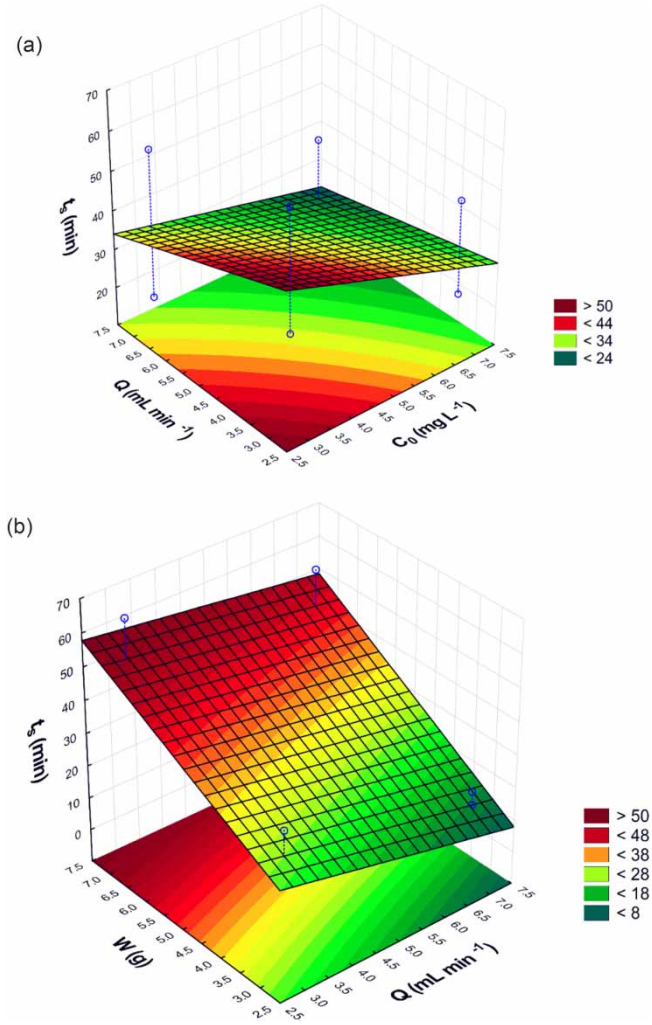

Figure 5 | Response surfaces of the saturation time of fixed-bed boron adsorption onto activated carbon as function of: (a) initial boron concentration and flow rate (W = 5 g); and (b) adsorbent weight and flow rate ($C_0 = 5$ mg L^{-1}).

The saturation time analysis

The following equation represents the regression model of saturation time (t_s), the time required to reach 95% of the initial concentration:

$$t_s = 34.54545 - 6.12500\,C_0 + 14.87500\,W - 5.12500\,Q - 2.37500\,C_0W + 1.12500\,C_0Q + 1.12500\,WQ \quad (18)$$

A high value for R^2, approximately 0.92181, indicates the model fits the experimental data well. Among the three variables of the study only adsorbent weight is significant in the statistical analysis (p-values <0.05, Table 5). However, initial boron concentration can be also significant due to its p-value closer to 0.05. Figure 5 shows the surface plots of the saturation time.

At high values of initial concentration, adsorption sites are filled more efficiently and the column saturation, 95% of C_0, is reached more quickly. This also demonstrates the gradient concentration has significant influence on the adsorption rate (Sotelo *et al.* 2013). Feed flow rate shows a negative effect on the saturation time. The saturation time decreased as the feed flow rate increased. At higher flow rates the residence time in the column is usually not long enough. In this case, the adsorbate molecule leaves the column before reaching the adsorption equilibrium (Chen *et al.* 2012). According to Figure 7(b), saturation time

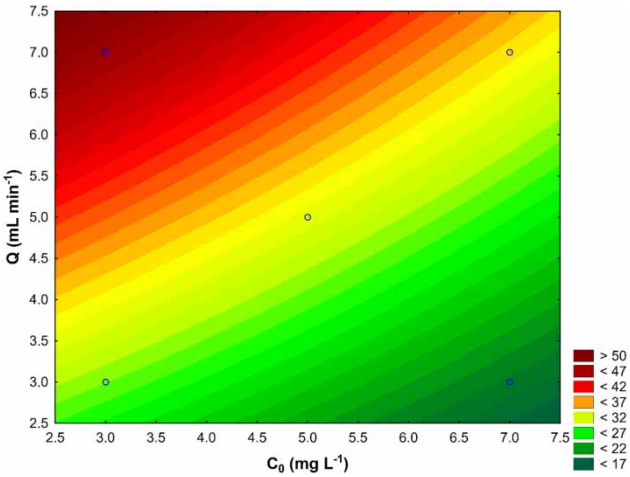

Figure 6 | Contour plot of the volume of effluent treated by the initial concentration of boron and flow rate (W = 5 g).

increased with increase in amount of adsorbent. At this condition, the number of binding sites is higher and the adsorbate has more time to diffuse through the pores of the adsorbent (Meng *et al.* 2013).

The volume of effluent treated analysis

Another response factor analyzed is the volume of effluent treated (V_S). The regression model for V_S is obtained with an R^2 of 0.890 and it is represented by the following equation:

$$V_s = 32.606 - 5.505\,C_0 + 1.541\,W + 8.208\,Q - 0.422\,C_0\,W - 0.827\,C_0\,Q + 3.791\,WQ \quad (19)$$

As can be observed in Table 5, the flow rate (Q) and initial boron concentration (C_0) are significant in the adsorption process, with *p*-values lower and closer to significance level of 0.05, respectively. The effects of these two variables are represented in the contour plot in Figure 6.

C_0 shows negative effect and Q shows positive effect on the volume of effluent treated. When flow rate decreases, less effluent is treated per gram of activated carbon. Lower inlet concentration causes slower transport of the boron molecules from the film layer to the adsorbent surface due to lower concentration gradient (de Franco *et al.* 2017).

The fractional bed utilization analysis

The FBU is a parameter which shows the fraction of packed column used for the adsorption process. Among the three variables of the study only adsorbent weight and flow rate

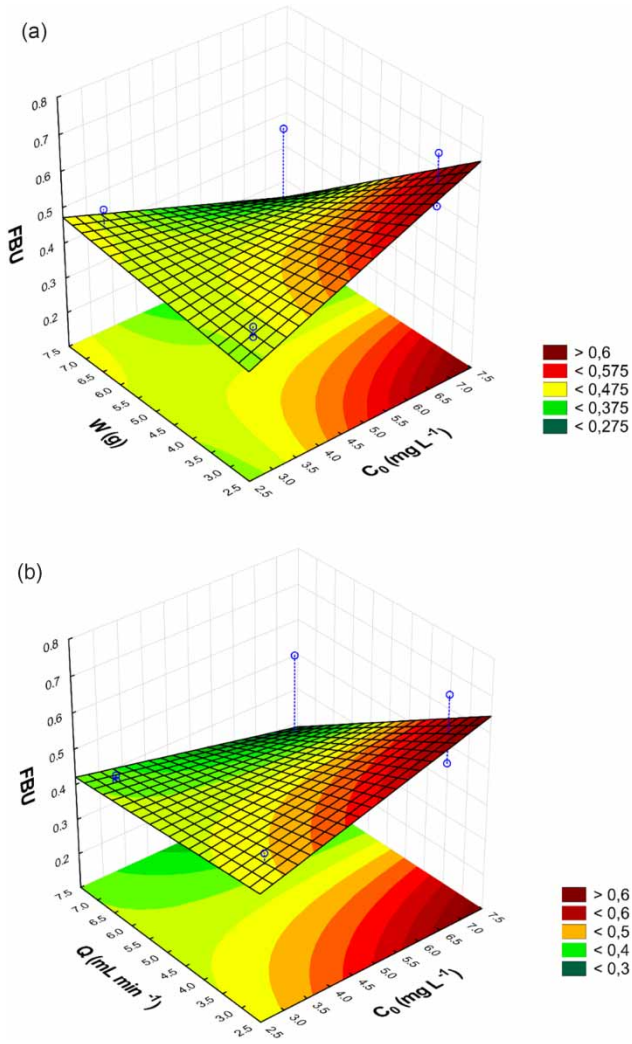

Figure 7 | Surface responses of the fractional bed utilization of fixed-bed boron adsorption onto activated carbon as function of: (a) initial boron concentration and adsorbent weight (Q = 5 mL min^{-1}) and (b) initial concentration and flow rate (W = 5 g).

are significant in the statistical analysis (*p*-values <0.05, Table 5). The following regression model is obtained using the real values:

$$\mathrm{FBU} = 0.452727 + 0.010875\,C_0 - 0.073125\,W - 0.079375\,Q - 0.079375\,C_0W - 0.051625\,C_0Q - 0.036125\,W \quad (20)$$

The determination coefficient value of 0.96081 indicates this equation explains about 96% of the variability in the response. Figure 7 shows two surfaces plots of FBU.

An increase in the initial concentration leads to higher FBU values. This result can be related to the fact that,

with more adsorbate molecules, the higher is the adsorption rate. On the other hand, the adsorbent weight shows negative effect on FBU. Even with higher amount of activated carbon, less of the bed is used for the adsorption process. Lower values of FBU are observed at higher amount of activated carbon due to the fact that not all of the adsorbent surface was accessible to molecules of the solute (Liao *et al.* 2013). It can be seen from Figure 7(b) that an increase in flow rate has a negative influence on the adsorption process. Higher values of FBU are observed at lower feed flow rates.

Mathematical modeling of the breakthrough curves

Traditional analytical models of Thomas, Bohart–Adams, Yoon–Nelson and Yan were employed to fit the breakthrough experimental data under different operation conditions of the experimental design. Model parameters and determination coefficients are shown in Table 6.

The Bohart–Adams model is suitable to reproduce the initial behavior of the breakthrough curve. In this case, the adjustment was carried out up to 50% of the initial concentration. The model was satisfactorily employed with an R^2 average of approximately 0.87. A good agreement of the experimental data to the Bohart–Adams model indicates that the surface diffusion is the rate-limiting step in the adsorption process (Calero *et al.* 2009). Both Thomas and Yan models were used to describe processes in which the external diffusion and intraparticle diffusion are not limiting stages of sorption (Chiavola *et al.* 2012). These models also consider the mass transfer at the solid surface as the limiting step. In addition, the adsorption equilibrium was represented by the Langmuir isotherm and has a reversible second-order kinetics (Mondal *et al.* 2016). The Yoon–Nelson model assumes that the rate of decrease in the probability of adsorption of the adsorbate molecules is directly proportional to the adsorbate molecule adsorption and the breakthrough of the adsorbent.

Among the four models tested, the Bohart–Adams model shows the lowest average of R^2, 0.672.

The breakthrough curve of boron at optimal point of the experimental design and the comparison between the adjustments to Thomas, Bohart–Adams, Yoon–Nelson and Yan models are shown in Figure 8.

The Yan model provides a better fit of the boron breakthrough curve compared to Thomas and Yoon–Nelson models due to its smoothly curved shape near the saturation zone. According to authors, the Yan model gives a better adjustment of experimental data by the fact this equation

Table 6 | Thomas, Bohart–Adams, Yoon–Nelson and Yan model parameters for boron adsorption by activated carbon at different operation conditions on fixed-bed column

Experimental conditions			Thomas model			Bohart–Adams model			Yan model			Yoon–Nelson model	
C_0 (mg L^{-1})	W (g)	Q (mL min^{-1})	K_{Th} (mL min^{-1} mg^{-1})	q_{Th} (mg g^{-1})	R^2	K_{BA} (m^3 mn^{-1} kg^{-1})	N_0 (kg m^{-3})	R^2	a_Y	q_Y (mg g^{-1})	R^2	K_{YN} (mL mn^{-1} mg^{-1})	R^2
7	7	7	0.077	33.305	0.993	9.302	0.0724	0.700	4.886	0.054	0.997	0.2706	0.993
3	3	7	140.990	0.018	0.999	10.843	45,325.809	0.608	5.099	0.017	0.997	0.49378	0.999
3	7	7	65.139	0.080	0.991	12.826	87,113.350	0.879	11.060	0.080	0.987	0.22813	0.991
7	3	7	0.346	6.535	0.980	4.413	46,409.549	0.305	3.684	0.006	0.992	1.21282	0.980
7	7	3	43.902	0.053	0.999	11.198	73,117.154	0.853	4.726	0.052	0.996	0.15374	0.996
7	3	3	0.239	14.377	0.986	5.083	63,961.175	0.471	6.457	0.014	0.989	0.8381	0.986
5	5	5	0.100	37.299	0.994	8.326	68,468.049	0.672	8.405	0.037	0.992	0.35166	0.994
5	5	5	0,105	37.335	0.995	8.349	68,423.899	0.668	8.747	0.037	0.993	0.36799	0.995
5	5	5	0.101	36.938	0.994	8.285	68,374.937	0.669	8.410	0.036	0.992	0.35541	0.994
3	7	3	0.059	92.167	0.994	9.831	104,239.229	0.850	11.507	0.091	0.994	0.20958	0.993
3	3	3	0.069	41.951	0.997	8.594	67,678.969	0.717	6.038	0.041	0.993	0.24247	0.997
Average					0.993			0.672			0.993		0.993

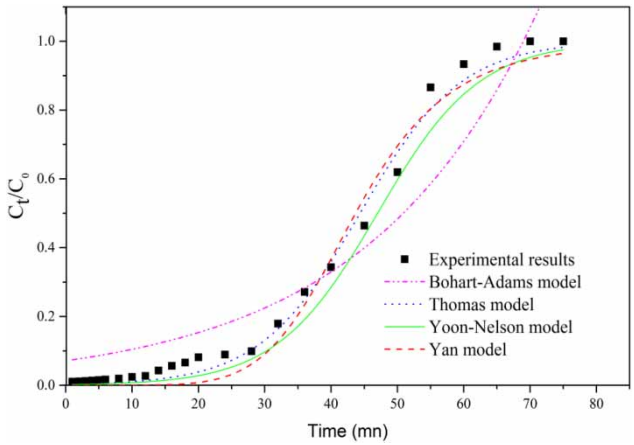

Figure 8 | Breakthrough curve of boron adsorption onto activated carbon in fixed-bed column ($C_0 = 3$ mg L^{-1}, W = 7 g, Q = 3 mL mn^{-1}).

minimizes the mathematical errors of the Thomas model (Chiavola *et al.* 2012).

The Yoon–Nelson model also showed a good correlation ($R^2 = 0.993$) with the experimental results. However, this model can be successfully applied for the boron adsorption on activated carbon to predict the breakthrough curves with insignificant deviations between model and experimental values.

The Thomas model assumes a Langmuir-type adsorption–desorption, isothermal and isobaric operating conditions, a constant column void fraction and second-order reversible kinetics (Meng *et al.* 2013). The Yan model could overcome the drawback of the Thomas model and both have the same considerations. In the 'Kinetic studies' section, it is observed that boron adsorption onto activated carbon followed more closely the pseudo-second-order equation than the pseudo-first-order model.

Furthermore, the equilibrium adsorption is better described by the Langmuir model compared to Freundlich. Both of these results are considerations of Yan and Thomas models than can relate batch adsorption with the fixed-bed column behavior. The three models of Yan, Thomas and Yoon–Nelson were suitable for the description of boron adsorption.

CONCLUSION

An activated carbon from palm bark is prepared and used for the removal of boron from aqueous medium. The activated carbon is characterized by FTIR spectroscopy, Brunauer–Emmett–Teller analysis, elemental analysis, Raman spectroscopy, pH_{pzc} method and X-ray diffraction analysis techniques. The experimental data are better correlated by the pseudo-second-order kinetic model rather than the pseudo-first-order kinetics. The equilibrium data are better described by the Langmuir and Sips models. The maximum adsorption capacity is 2.377 mg g^{-1}. The thermodynamic results show the exothermic nature of adsorption of boron on activated carbon. Fixed-bed adsorption experiments reveal that initial boron concentration, adsorbent dosage and flow rate affected both breakthrough and saturation times. Mathematical models for the breakthrough curves are successfully applied. The Yan model fitted better the experimental data of all tests than other models ($R^2$0.993) while the Thomas model is the best equation for the prediction of boron adsorption capacity (q_{TH}). Based on the results, it can be concluded that the activated carbon is an effective adsorbent for the removal of boron from aqueous medium.

REFERENCES

Abdu, S., Martí-Calatayud, M. C., Wong, J. E., García-Gabaldón, M. & Wessling, M. 2014 Layer-by-layer modification of cation exchange membranes controls ion selectivity and water splitting. *American Chemical Society: Applied Materials & Interfaces* **6** (3), 1843–1854.

Ahmad, A. A. & Hameed, B. H. 2010 Fixed-bed adsorption of reactive azo dye onto granular activated carbon prepared from waste. *Journal of Hazardous Materials* **175** (1–3), 298–303.

Anderson, M. J. & Whitcomb, P. J. 2005 *RSM Simplified: Optimizing Processes Using Response Surface Methods for Design of Experiments*, 2nd edn. Taylor & Francis, New York, USA

Bakkal, G. C., Bilgin, S. E., Duranoglu, D. & Beker, U. 2015 An experimental design approach for modeling As(V) adsorption from aqueous solution by activated carbon. *Water Science & Technology* **71** (2), 203–210.

Bohart, G. S. & Adams, E. Q. 1920 Some aspects of the behavior of charcoal with respect to chlorine. *Journal of the American Chemical Society* **42** (3), 523–544.

Calero, M., Hernáinz, F., Blázquez, G., Tenorio, G. & Martín-Lara, M. A. 2009 Study of Cr(III) biosorption in a fixed-bed column. *Journal of Hazardous Materials* **171** (1–3), 886–893.

Chen, S., Yue, Q., Gao, B., Li, Q., Xu, X. & Fu, K. 2012 Adsorption of hexavalent chromium from aqueous solution by modified corn stalk: a fixed-bed column study. *Bioresource Technology* **113**, 114–120.

Chiavola, A., D'Amato, E. & Baciocchi, R. 2012 Ion exchange treatment of groundwater contaminated by arsenic in the presence of sulphate. Breakthrough experiments and modeling. *Water, Air, & Soil Pollution* **223** (5), 2373–2386.

Cruz-Olivares, J., Pérez-Alonso, C., Barrera-Díaz, C., Ureña-Nuñez, F., Chaparro-Mercado, M. C. & Bilyeu, B. 2013 Modeling of lead (II) biosorption by residue of allspice in a fixed-bed column. *Chemical Engineering Journal* **228**, 21–27.

Danmaliki, G. I. & Saleh, T. A. 2016 Influence of conversion parameters of waste tires to activated carbon on adsorption of dibenzothiophene from model fuels. *Journal of Cleaner Production* **117**, 50–55.

de Franco, M. A. E., de Carvalho, C. B., Bonetto, M. M., de Pelegrini, S. R. & Féris, L. A. 2017 Removal of amoxicillin from water by adsorption onto activated carbon in batch process and fixed bed column: kinetics, isotherms, experimental design and breakthrough curves modelling. *Journal of Cleaner Production* **161**, 947–956.

Dydo, P., Nemś, I. & Turek, M. 2012 Boron removal and its concentration by reverse osmosis in the presence of polyol compounds. *Separation and Purification Technology* **89**, 171–180.

Foo, K. Y. & Hameed, B. H. 2012 Textural porosity, surface chemistry and adsorptive properties of durian shell derived activated carbon prepared by microwave assisted NaOH activation. *Chemical Engineering Journal* **187**, 53–62.

García-Mateos, F. J., Ruiz-Rosas, R., Marqués, M. D., Cotoruelo, L. M., Rodríguez-Mirasol, J. & Cordero, T. 2015 Removal of paracetamol on biomass-derived activated carbon: modeling the fixed bed breakthrough curves using batch adsorption experiments. *Chemical Engineering Journal* **279**, 18–30.

Georgieva, V. G., Tavlieva, M. P., Genieva, S. D. & Vlaev, L. T. 2015 Adsorption kinetics of Cr(VI) ions from aqueous solutions onto black rice husk ash. *Journal of Molecular Liquids* **208**, 219–226.

Ho, Y. S. & McKay, G. 1999 Pseudo-second order model for sorption processes. *Process Biochemistry* **34** (5), 451–465.

Hsu, S. H., Huang, C. S., Chung, T. W. & Gao, S. 2014 Adsorption of chlorinated volatile organic compounds using activated carbon made from *Jatropha curcas* seeds. *Journal of the Taiwan Institute of Chemical Engineers* **45** (5), 2526–2530.

Islam, M. A., Tan, I. A. W., Benhouria, A., Asif, M. & Hameed, B. H. 2015 Mesoporous and adsorptive properties of palm date seed activated carbon prepared via sequential hydrothermal carbonization and sodium hydroxide activation. *Chemical Engineering Journal* **270**, 187–195.

Kavitha, D. 2016 Adsorptive removal of phenol by thermally modified activated carbon: equilibrium, kinetics and thermodynamics. *Journal of Environment & Biotechnology Research* **3** (1), 24–34.

Lagergren, S. 1898 Zur Theorie der sogenannten Adsorption geloster Stoffe. *Kungliga Svenska Vetenskapsakademiens Handlingar* **24**, 1–39.

Liao, P., Zhan, Z., Dai, J., Wu, X., Zhang, W., Wang, K. & Yuan, S. 2013 Adsorption of tetracycline and chloramphenicol in aqueous solutions by bamboo charcoal: a batch and fixed-bed column study. *Chemical Engineering Journal* **228**, 496–505.

Liu, H., Ye, X., Li, Q., Kim, T., Qing, B., Guo, M., Ge, F., Wu, Z. & Lee, K. 2009 Boron adsorption using a new boron-selective hybrid gel and the commercial resin D564. *Colloids and Surfaces A: Physicochemical and Engineering Aspects* **341** (1–3), 118–126.

Lyu, J., Zhang, N., Liu, H., Zeng, Z., Zhang, J., Bai, P. & Guo, X. 2017 Adsorptive removal of boron by zeolitic imidazolate framework: kinetics, isotherms, thermodynamics, mechanism and recycling. *Separation and Purification Technology* **187**, 67–75.

Mahmood, T., Ali, R., Naeem, A., Hamayun, M. & Aslam, M. 2017 Potential of used *Camellia sinensis* leaves as precursor for activated carbon preparation by chemical activation with H_3PO_4; optimization using response surface methodology. *Process Safety and Environmental Protection* **109**, 548–563.

Meng, M., Feng, Y., Zhang, M., Liu, Y., Ji, Y., Wang, J., Wu, Y. & Yan, Y. 2013 Highly efficient adsorption of salicylic acid from aqueous solution by wollastonite-based imprinted adsorbent: a fixed-bed column study. *Chemical Engineering Journal* **225**, 331–339.

Mondal, S., Aikat, K. & Halder, G. 2016 Ranitidine hydrochloride sorption onto superheated steam activated biochar derived from mung bean husk in fixed bed column. *Journal of Environmental Chemical Engineering* **4** (1), 488–497.

Saha, P. & Chowdhury, S. 2011 Insight into adsorption thermodynamics. *Thermodynamics*. IntechOpen. doi:10.5772/13474.

Shaaban, M. M. 2010 Role of boron in plant nutrition and human health. *American Journal of Plant Physiology* **5** (5), 224–240.

Shaidan, N. H., Eldemerdash, U. & Awad, S. 2012 Removal of Ni(II) ions from aqueous solutions using fixed-bed ion exchange column technique. *Journal of the Taiwan Institute of Chemical Engineers* **43**, 40–45.

Sotelo, J. L., Ovejero, G., Rodríguez, A., Álvarez, S. & García, J. 2013 Analysis and modeling of fixed bed column operations on flumequine removal onto activated carbon: pH influence and desorption studies. *Chemical Engineering Journal* **228**, 102–113.

Sulaiman, N. S., Hashim, R., Amini, M. H. M., Danish, M. & Sulaiman, O. 2018 Optimization of activated carbon preparation from cassava stem using response surface methodology on surface area and yield. *Journal of Cleaner Production* **198**, 1422–1430.

Thomas, H. C. 1944 Heterogeneous ion exchange in a flowing system. *Journal of American Chemical Society* **66** (10), 1664–1666.

Torrellas, S. Á., García Lovera, R., Escalona, N., Sepúlveda, C., Sotelo, J. L. & García, J. 2015 Chemical-activated carbons from peach stones for the adsorption of emerging contaminants in aqueous solutions. *Chemical Engineering Journal* **279**, 788–798.

Yan, G. & Viraraghavan, T. 2003 Heavy-metal removal from aqueous solution by fungus *Mucor rouxii*. *Water Research* **37** (18), 4486–4496.

Zuorro, A. 2015 Optimization of polyphenol recovery from espresso coffee residues using factorial design and response surface methodology. *Separation and Purification Technology* **152**, 64–69.

First received 16 October 2019; accepted in revised form 27 February 2020. Available online 9 March 2020